Volume 2, 2026, Pages 139-149 *Journal of Smart and Sustainable Farming*
| Regular Article | Open Access

Thermal Imaging Based Assessment of Livestock Heat Stress for Climate Resilient Farm Management

Zengling Wang
Agricultural Engineering, College of Engineering, China Agricultural University, Beijing 100083, China.
yangzengling26@gmail.com

Article Info
Journal of Smart and Sustainable Farming
https://www.ansispublications.com/jssf/jssf.html

© The Author(s), 2026.
https://doi.org/10.64026/JSSF/2026012

Received 25 March 2026
Revised from 30 April 2026
Accepted 06 June 2026
Available online 30 June 2026
Published by Ansis Publications.

Corresponding author(s):
Zengling Wang, Agricultural Engineering, College of Engineering, China Agricultural University, China.
Email: yangzengling26@gmail.com

This article is an open access article distributed under the terms and conditions of the Creative Commons Attribution (CC BY) license (https://creativecommons.org/licenses/by/4.0/).

Abstract – With the rising temperatures and humidity, the frequency and intensity of heat stress is affecting the productivity, animal welfare and profitability of farms. Environmental conditions are traditionally described by the temperature–humidity index (THI) and this index do not fully describe the physiological responses of the individual. Rectal thermometry, on the other hand, is a good reference measurement, but it is invasive, time consuming, and not suitable for continuous monitoring of a herd. The present study aims to propose a framework for infrared thermography (IRT) for non-invasive assessment of heat stresses in dairy cattle based on radiometric correction, automated body segmentation, region-of-interest (ROI) detection, thermal feature extraction, and machine-learning classification, and to integrate the barn microclimate measurements into this framework. The framework was tested with 120 animal-sessions ranging between THI 65.8 to 89.6. The overall performance of Otsu based Segmentation was good in extracting the animal regions, with an intersection-over-union (IoU) score of 0.95. The maximum eye temperature had a high correlation with the rectal temperature ($r = 0.92$) and RMSE of 0.15 °C. The logistic regression classifier that integrated eye temperature and THI had an accuracy of 0.84 and an area under the receiver operating characteristic curve (AUC) of 0.92 to identify heat stressed animals based on the criterion of rectal temperature ≥ 39.2 °C. The benefit of adding animal level thermal information was demonstrated by comparing with THI-only classification that had an AUC of 0.75. In addition, a 24-hour monitoring system detected an average delay of 2.25 hours between changes in THI and change in herd eye-temperature. This temporal relationship can be used to make pre-emptive cooling decisions. The proposed framework provides multiple levels of alerts for shade, sprinkler and ventilation management, providing a practical way to improve climate resilient livestock production, animal welfare and even resource utilisation.

Keywords – Infrared Thermography, Heat Stress, Dairy Cattle, Temperature–Humidity Index, Image Segmentation, Precision Livestock Farming, Climate Resilience.

I. INTRODUCTION

Thermal stress in livestock is being exacerbated by climate change through its effect on ambient temperature, humidity and the occurrence of extreme heat events. Dairy cattle are especially susceptible to heat stress as their heat load is caused by metabolic heat production and/or environmental heat load, compared to their physiological capacity for dissipating heat. Thermal stress increases feed intake, decreases milk production, impacts reproductive performance, impairs immune function, and impacts animal welfare. The impacts can negatively affect a farm's profitability and undermine the sustainability of livestock farming, especially in tropical and subtropical countries where high temperatures and humidity stay for long periods. Therefore, the development of reliable and timely heat stress assessment methods is crucial for effective and sustainable farm management under climate change. These techniques should be able to detect physiological stress before negative consequences arise and should give information to take appropriate action to implement cooling strategies [1].

Environmental heat load is often expressed in terms of the temperature–humidity index (THI) used in livestock systems. It integrates ambient temperature and relative humidity into one indicator for identifying potentially stressful environmental conditions. But the only thing THI indicates and does not measure, is the external environment of the animals. Variations in breed, age, stage of lactation, body condition, acclimatization and individual thermoregulatory response can give rise to different responses to similar environmental conditions. Also, THI can be a poor indicator of the effects of solar radiation, air movement, housing and accumulated heat exposure effects. Therefore, solely using environmental indicators could lead to inaccurate or not earlier detection of animals with high body temperature. Combination of physiological indices at the animal level with environmental measurements therefore can offer a more holistic perspective on heat stress assessment [2].

Rectal temperature is often used as a reference point for assessing the temperature of cattle. It can give important physiological information, but it will only be used in routine use if the animal needs to be handled, trained staff is available and measurements need to be repeated. These requirements can contribute to higher labour costs, disruptions to normal animal behaviour, and reduce the practicality of continuous monitoring in large herds. Furthermore, periodic measurements may not reflect the immediate changes of temperature and physiological response to the altered environmental conditions. The restrictions that have been imposed lead to the development of non-invasive tools that allow the measurement of the thermal response of animals with minimal disturbance. Infrared thermography (IRT) is a promising alternative since it can be used to capture the temperature distribution of the surfaces without a direct contact. IRT measures thermal radiation from the animal's body, allowing the identification of temperature differences in specific anatomical areas that can reflect changes in the control of thermoregulation [3].

Although it has potential application, there are important issues to consider when applying IRT in livestock environments: image acquisition, environmental interference, anatomical localization, and temperature measurement accuracy. Thermal values may be affected by distance from the camera, angle of view, emissivity, background temperature, wetness of surfaces and animal movement. Manual delineation of anatomical regions can also be cumbersome and subject to operator dependent variability. Thus, an automated processing pipeline is required to increase consistency and ease of scale deployment. The reliability of temperature measurement can be enhanced by radiometric correction, and the image pre-processing can be used to reduce noise and highlight more prominent thermal structures. Isolate an animal from background using segmentation techniques such as Otsu thresholding and body-mask extraction using U-Net. Object detection technique like You Only Look Once (YOLO) can then detect Regions of Interest (ROIs) like eyes, muzzles and flanks, which allows for systematic extraction of anatomically relevant temperature features [4].

In addition to temperature measurement, a cluster of thermal characteristics and environmental factors could enhance the differentiation between normal and heat stressed animals. The eye temperature has been of special interest due to its relationship to changes in physiology that occur under stress and thermoregulatory conditions. But surface temperature is not necessarily a reliable indicator of internal temperature in all situations. Maximum eye temperature, combined with THI and other thermal descriptors, such as thermal stability index (TSI) and temperature differences (ΔT) can offer complementary information regarding the response of animals and the heat load of the environment. These relationships can be leveraged using machine-learning techniques to estimate physiological temperature and classify heat stress conditions. The regression models can be used to estimate thermal responses, and logistic classification models can be used to classify animals into pre-defined thermal stress categories from the combination of thermal and microclimatic features [5].

A second key issue is the time lag between exposure to environmental heat and the response of the animal's physiology. When environmental factors start to shift, cattle may persist in accumulating body heat and physiological recovery may not be complete at night after extended daytime exposure. Therefore, the use of only a single threshold for the THI could not accurately capture the changing thermal status of the herd. Repeated IRT monitoring and/or barn microclimate monitoring can be used to help identify response delay and recovery patterns. Such information can support tiered decision-making, including timely activation of shade, sprinklers, and ventilation, while avoiding unnecessary water and energy consumption. Integrating these outputs into a farm decision-support framework can strengthen climate adaptation and improve resource efficiency [6].

Against this background, this study proposes an IRT-based framework for non-invasive cattle heat-stress assessment and climate-resilient farm management. The framework integrates radiometric correction, automated segmentation, ROI-based thermal feature extraction, environmental THI measurements, and machine-learning-based prediction. Its objectives are to evaluate segmentation performance, examine the relationship between eye temperature and rectal temperature, compare combined thermal–environmental classification against THI-only assessment, and investigate temporal patterns relevant to cooling decisions. The framework is evaluated using a demonstration dataset comprising 120 animal-sessions across THI values ranging from 65.8 to 89.6. By linking animal-level thermal measurements with environmental conditions and actionable management outputs, this work aims to establish a practical foundation for scalable livestock heat-stress monitoring. The resulting approach is intended to support early intervention, animal welfare, and resource-efficient dairy production under increasingly variable climatic conditions [7].

II. RELATED WORKS

Infrared thermography (IRT) has proven to be a promising non-invasive technique for assessing the thermal response, physiology and welfare in animals. Measuring physiological traits such as rectal temperature or respiratory-rate using conventional methods, however, is important and requires animal handling and repeated manual observations. The non-invasive physiological responses to heat stress in cattle, singling out IRT as a potentially useful tool for quick assessment of heat stress, and highlighting the need for standardisation of measurement procedures and reliable heat stress thresholds. Likewise, the use of IRT for assessing thermal responses in livestock and the necessity of anatomical measurement area and thermal environment [8].

There have been several experimental studies that have explored the link between core body temperature and surface temperature. In [9] the researchers analyzed video-based IR temperature readings of cows and calves, and suggested that the eye and ear regions were good targets for practical temperature monitoring. In [10] the authors tested 488 Holstein dairy cows and reported that the surface temperature changes with the environment heat load (THI). They also found that the relationships varied from one anatomical region to another, illustrating the need for appropriate thermal windows.

Table 1. Comparative Analysis of Existing Studies on IRT-Based Livestock Heat-Stress Assessment

Ref.	Method / focus	Main contribution	Identified limitation
[7]	Review of non-invasive physiological indicators	Identified IRT as a promising rapid indicator of cattle heat stress.	Standardized thresholds and measurement protocols remain necessary.
[8]	Review of IRT-based thermal assessment	Discussed physiological responses and thermal measurement regions.	Thermal responses vary with species, region, and experimental conditions.
[9]	Video-based infrared thermography	Identified eye and ear regions as practical temperature-monitoring locations.	Limited animal sample and dependence on measurement conditions.
[10]	IRT and rectal-temperature measurements in 488 Holstein cows	Demonstrated variation in surface temperature under different THI conditions.	Anatomical regions differ in their ability to represent core temperature.
[11]	Thermal imaging of Nellore cattle	Investigated associations between body-region temperatures, rectal temperature, and respiratory frequency.	Focused on thermal physiology and feed efficiency rather than automated heat-stress classification.
[12]	Thermal and physiological biomarker analysis	Examined relationships between heat stress, surface temperature, and physiological indicators.	Requires integration into automated, real-time farm decision support.
[13]	Review of livestock thermal-imaging applications	Summarized temperature measurement, disease detection, and thermoregulation applications.	Primarily reviews existing methods rather than implementing a unified cattle monitoring pipeline.
[14]	Review of IRT and machine learning	Examined opportunities for machine-learning-assisted interpretation of cattle thermal data.	Automated, integrated farm-level heat-stress decision support remains a development need.
[15]	Ocular temperature and environmental-variable regression	Demonstrated the potential to estimate rectal temperature using ocular and ambient measurements.	Results are species-specific and require further validation across production conditions.
[16]	Infrared skin-temperature measurements under controlled heat exposure	Investigated skin temperature as a potential alternative indicator of thermal stress.	Small experimental sample and limited automated classification capabilities.

The study of IRT under tropical production conditions has also been the subject of research. In [11] the authors studied thermal measurements in Nellore cattle and established relationships between temperatures of different parts of the body, rectal temperature and respiratory frequency. The authors in [12] studied body-surface temperatures in addition to metabolic, endocrine, and inflammatory responses in heat-stressed cows, which demonstrates the importance of combining thermal data with other physiological data. These studies validate the application of animal-level thermal indicators but also show how to use surface temperature in conjunction with environmental and physiological factors.

New possibilities with automation and machine learning to enhance IRT-based monitoring consistency and scaling. In [13] reviewed the use of IRT in livestock and poultry, such as temperature measurement, disease detection and assessment of thermoregulation. The authors in [14] conducted an independent analysis of IRT and machine-learning applications for livestock health evaluation, exploring automated IRT data interpretation. All these developments prompt to incorporate image processing, anatomical region detection, feature extraction and predictive modelling in a single pipeline.

Recently buffaloes have also been studied in terms of regression analysis for the estimation of core body temperature from ocular temperature and environmental parameters. The results reported show that the use of animal level thermal data in combination with environmental variables can be helpful in creating predictive information, but the usefulness of this information depends on the type of species and experimental conditions [15]. Moreover, the study [16] on infrared skin-temperature measurements as heat stress or animal welfare indicators confirmed the importance of assessing thermal measurements in addition to known thermal measures.

However, there are significant limitations in the integration of the use of radiometric correction, automated segmentation, multiple thermal features, THI-based environmental measurements and machine-learning classification into a single farm decision-support framework. This research gap is addressed here by integrating eye temperature (from IRT) with THI, testing classification against a rectal-temperature-based reference, and research into temporal response patterns for cooling management. It focuses on the monitoring of heat stress, as well as the implementation of farm interventions that are cost effective and resource efficient. **Table 1** shows Comparative Analysis of Existing Studies on IRT-Based Livestock Heat-Stress Assessment

III. MATERIALS AND METHODS

Overall Framework

The framework (**Fig. 1**) comprises six stages: data acquisition, radiometric pre-processing, segmentation, feature extraction, heat-stress modelling and farm decision support. A feedback loop recalibrates the models against reference core-temperature measurements and weather forecasts.

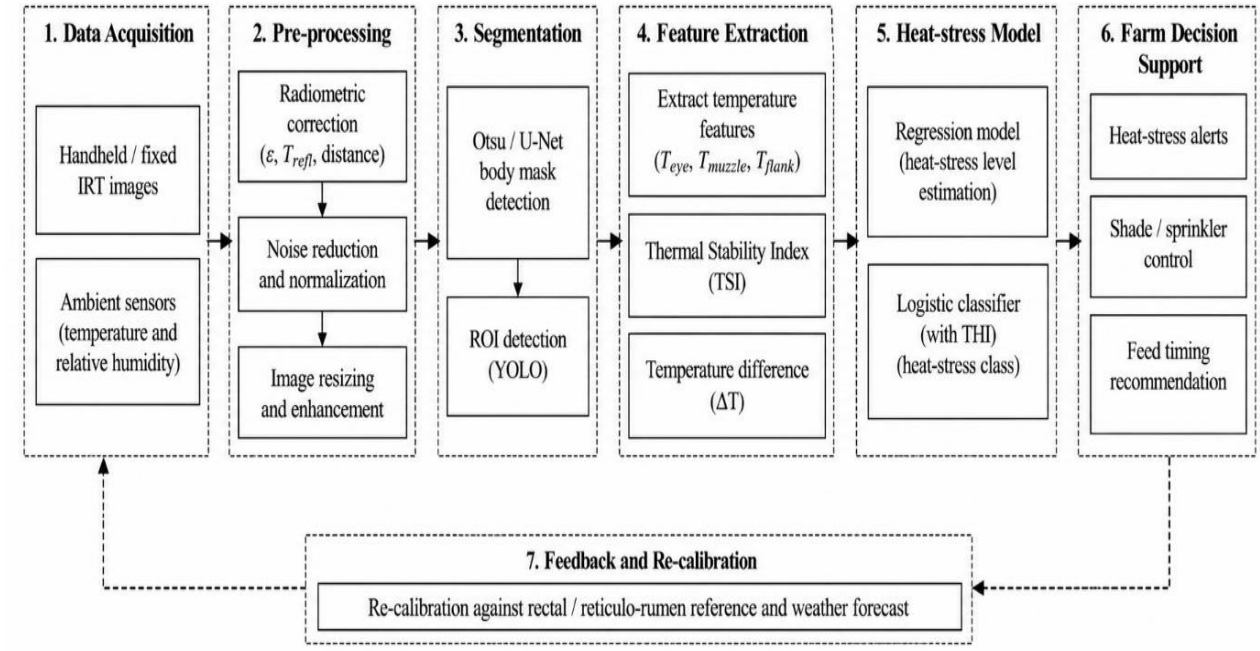


Fig 1. Proposed IRT-Based Framework for Heat-Stress Assessment and Decision Support.

The conceptual framework shown here is a systematic pipeline for non-invasive cattle heat stress assessment based on infrared thermography (IRT) and environmental measurements. During the data acquisition stage the IRT images and ambient temperature and relative humidity are captured using handheld or fixed camera. Pre-processing includes radiometric correction, noise reduction, normalization and image enhancement, which improves the quality of the data. In the segmentation stage, Otsu thresholding or U-Net is used for body-mask detection, and YOLO is used for the region-of-interest (ROI) identification. Subsequently, feature extraction involves calculating eye, muzzle and flank temperatures, the Thermal Stability Index (TSI), and temperature differences (ΔT). The heat-stress modelling phase combines the regression-based model of stress levels with logistic classification based on the Temperature–Humidity Index (THI). Predictions are used to aid in heat-stress alerts, shade and sprinkler control, and in optimizing feeding times. Reference measurements and weather forecasts are used to ensure the reliability of the model when the environment changes, as such they are included in a feedback and recalibration loop.

Animals, Site and Data Acquisition

The study design covers 40 lactating crossbred dairy cows housed in a naturally ventilated free-stall barn and imaged in three sessions under contrasting thermal conditions (early morning, midday and afternoon), giving 120 animal-sessions. Lateral thermograms of the standing animal were captured from 3–4 m, perpendicular to the body, with a handheld radiometric camera (320 × 240 pixels, NETD ≤ 50 mK, accuracy ±2 °C or ±2 %; [replace with your camera model]), out

of direct sunlight and with the eye, muzzle and flank visible. Immediately afterwards, rectal temperature (T_{rec}) was recorded with a digital clinical thermometer and respiration rate (RR) was counted over 60 s from flank movement. Dry-bulb temperature (T_{db}) and relative humidity (RH) were logged at animal height every 5 min. An animal was classified as heat-stressed when $T_{rec} \geq 39.2$ °C, a commonly used upper limit of normal body temperature in cattle. Barn microclimate was expressed as THI [6]:

$$\mathrm{THI} = 0.8\mathrm{T_{db}} + \frac{\mathrm{RH}}{100}(\mathrm{T_{db}} - 14.4) + 46.4 \tag{1}$$

Radiometric Correction

Raw camera output is an apparent radiometric temperature that depends on target emissivity (ε), reflected ambient radiation and atmospheric attenuation [13]. Over short distances (< 5 m) attenuation is negligible, so the object temperature (in kelvin) was estimated from the apparent temperature T_{rad} and the reflected apparent temperature T_{refl}, measured with a crumpled-foil reflector, as

$$\mathrm{T_{obj}} = \sqrt[4]{\frac{\mathrm{T_{rad}^4} - (1-\varepsilon)\mathrm{T_{refl}^4}}{\varepsilon}} \tag{2}$$

An emissivity of ε = 0.98 was used for hair-covered skin and the eye, which behave as near-blackbody surfaces in the long-wave infrared band. Frames were exported as 16-bit radiometric matrices rather than colour-palette images so that each pixel retained a temperature value.

Body Segmentation and ROI Extraction

The animal was separated from the background with Otsu's method [14], which selects the threshold t^* that maximises the between-class variance of the temperature histogram:

$$\sigma_B^2(t) = \omega_0(t)\omega_1(t)[\mu_0(t) - \mu_1(t)]^2 \tag{3}$$

$$t^* = \arg\max_t \sigma_B^2(t) \tag{4}$$

Here ω_0, ω_1 and μ_0, μ_1 are the class probabilities and mean temperatures below and above t. The binary mask was cleaned by morphological closing and removal of small connected components. The ROIs—eye (maximum temperature of the medial canthus region), muzzle, flank (mean of a fixed rectangle over the lateral abdomen) and lower limbs—were located by a YOLO-type detector [16] in the production system and by geometric landmarks relative to the mask in this study. A U-Net [15] is the recommended alternative where backgrounds are thermally cluttered and simple thresholding fails. Segmentation quality was measured by intersection over union (IoU), where A is the predicted and B the reference mask:

$$\mathrm{IoU} = \frac{|A \cap B|}{|A \cup B|} \tag{5}$$

Thermal Indices and Statistical Modelling

Maximum eye temperature (T_{eye}) was the primary indicator because the eye region is richly vascularised, has little hair and is less affected by coat condition. To compare animals across sessions, a thermal stress index (TSI) was defined as the standardised deviation of T_{eye} from the thermoneutral baseline (sessions with THI < 72; n = 36, mean 34.35 °C, SD 0.33 °C):

$$\mathrm{TSI} = \frac{\mathrm{T_{eye}} - \mu_{\mathrm{TN}}}{\sigma_{\mathrm{TN}}} \tag{6}$$

Core temperature was estimated by multiple linear regression on T_{eye} and THI,

$$\mathrm{T_{rec}} = \beta_0 + \beta_1 \mathrm{T_{eye}} + \beta_2 \mathrm{THI} + \varepsilon \tag{7}$$

and the probability of heat stress (HS) was modelled by logistic regression with standardised predictors,

$$\mathrm{P(HS = 1)} = \frac{1}{1 + e^{-(\gamma_0 + \gamma_1 \mathrm{T_{eye}} + \gamma_2 \mathrm{THI})}} \tag{8}$$

Both models were evaluated by stratified five-fold cross-validation. Estimation error was summarised by the root-mean-square error,

$$\mathrm{RMSE} = \sqrt{\frac{1}{\mathrm{n}} \sum_{\mathrm{i=1}}^{\mathrm{n}} \left(\mathrm{T_{rec,i}} - \mathrm{T_{est,i}}\right)^2} \tag{9}$$

and classification by accuracy, precision (P), recall (R), the area under the receiver operating characteristic curve (AUC) and the F1 score:

$$F_1 = \frac{2PR}{P+R}, \quad P = \frac{TP}{TP+FP}, \quad R = \frac{TP}{TP+FN} \tag{10}$$

Agreement between IRT-estimated and rectal temperature was assessed by Bland–Altman analysis (bias and 95 % limits of agreement).

IV. RESULTS AND DISCUSSION

Thermal Signatures of Heat Stress

Fig. 2 shows representative thermograms under thermoneutral, moderate and severe heat conditions, with the automatically placed ROIs, and **Table 2** lists the mean ROI temperatures. As ambient temperature rose by 14.5 °C, the eye and flank ROIs warmed by 3.8 and 4.2 °C, respectively, whereas the lower limbs warmed by 10.1 °C, almost in step with the environment. Eye and trunk temperature are therefore buffered by thermoregulation and reflect the animal's physiological state, while the extremities behave largely as passive thermometers of the surroundings. The muzzle remained the coolest of the head and trunk ROIs, consistent with evaporative cooling from moist skin. The eye–flank gradient narrowed from 1.6 °C to 1.2 °C as peripheral vasodilation raised skin temperature towards core temperature.

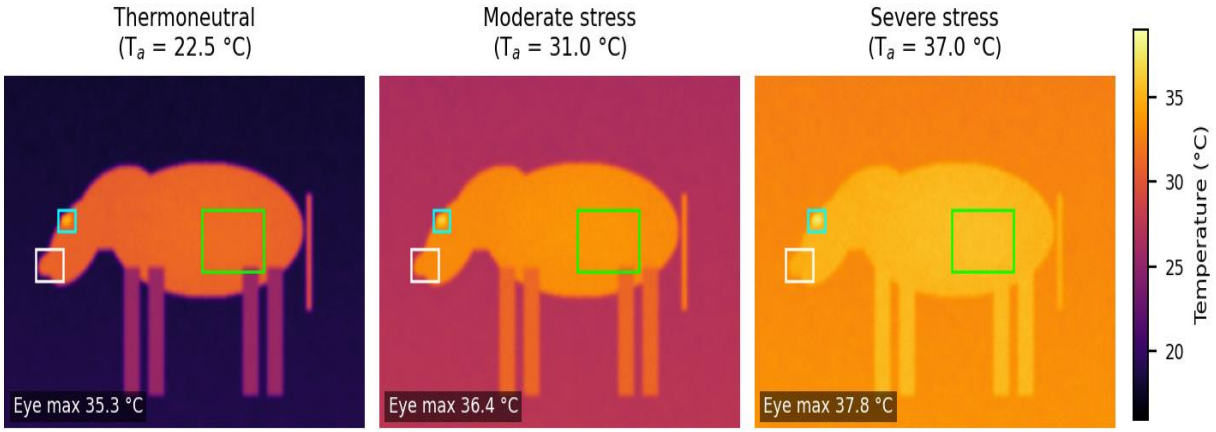


Fig 2. Simulated Radiometric Thermograms of a Cow Under Thermoneutral, Moderate and Severe Heat Conditions. Boxes Mark the Eye (Cyan), Muzzle (White) and Flank (Green) Rois; The Colour Scale is Common to All Panels.

Table 2. Mean ROI Temperatures (°C) Extracted from the Thermograms in **Fig. 2**.

Sample	Condition	(T_a) (°C)	Eye (°C)	Muzzle (°C)	Flank (°C)	Lower limbs (°C)
1	Thermoneutral	22.5	33.0	30.1	31.4	25.1
2	Thermoneutral	23.0	33.2	30.3	31.6	25.4
3	Thermoneutral	23.5	33.4	30.5	31.8	25.7
4	Moderate stress	29.0	34.5	32.0	33.0	29.8
5	Moderate stress	30.0	34.8	32.3	33.3	30.3
6	Moderate stress	31.0	35.0	32.6	33.6	30.9
7	Moderate stress	32.0	35.3	32.9	33.9	31.3
8	Severe stress	35.0	36.0	34.0	34.9	34.0
9	Severe stress	36.0	36.4	34.4	35.3	34.6
10	Severe stress	37.0	36.8	34.7	35.6	35.2

Segmentation and ROI Extraction

Fig. 3 illustrates the processing chain on the moderate-stress frame. Otsu's method returned a threshold of 29.9 °C, which cleanly separated the warm body from the cooler barn background; after morphological clean-up the mask achieved an IoU of 0.95 and a Dice coefficient of 0.97 against the reference mask. Because the segmentation operates on temperature rather than colour, it is insensitive to lighting, which is an advantage over visible-light computer vision in barns. Its weakness is contrast: when the background is close to skin temperature, for example sun-warmed walls on a hot afternoon, a single global threshold fails. In such cases a shaded, thermally neutral backdrop at the milking or feeding station, or a learned U-Net segmenter [15], is advisable.

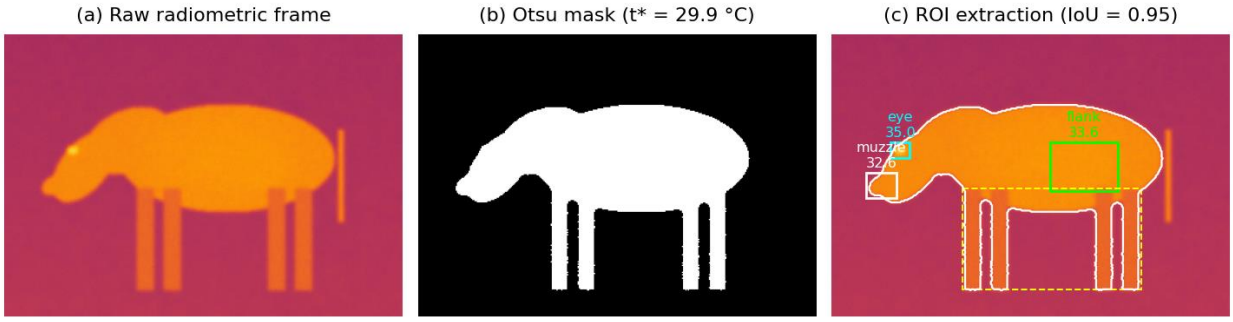


Fig 3. Image-Processing Pipeline on a Simulated Frame: (A) Raw Radiometric Frame, (B) Otsu Body Mask and (C) Mask Contour with Extracted Rois and Their Mean Temperatures (°C).

Relationship Between IRT, THI and Rectal Temperature

Across the 120 animal-sessions, THI ranged from 65.8 to 89.6 and 32 sessions (27 %) met the heat-stress criterion. Rectal temperature averaged 39.41 °C in stressed and 38.77 °C in non-stressed animals, while T_{eye} averaged 35.36 and 34.65 °C; the corresponding mean TSI was 3.06 versus 0.90. Eye temperature was the best single predictor of rectal temperature (r = 0.92), clearly ahead of flank temperature (r = 0.65) and THI (r = 0.62), and was also correlated with respiration rate (r = 0.67). Simple regression gave $T_{rec} = 13.75 + 0.723T_{eye}$ (cross-validated R^2 = 0.85, RMSE = 0.15 °C; **Fig. 4a**). Adding THI as in Eq. (7) improved cross-validated R^2 only marginally, to 0.87 (RMSE = 0.14 °C; β_2 = -0.013), because the effect of the environment on core temperature is already expressed through the eye temperature. The Bland–Altman plot **(Fig. 4b)** shows negligible bias (0.00 °C) and 95 % limits of agreement of ±0.30 °C without a visible trend with temperature, which is within the ±0.3–0.5 °C tolerance commonly accepted for clinical temperature screening and well below the 0.7 °C separation between group means.

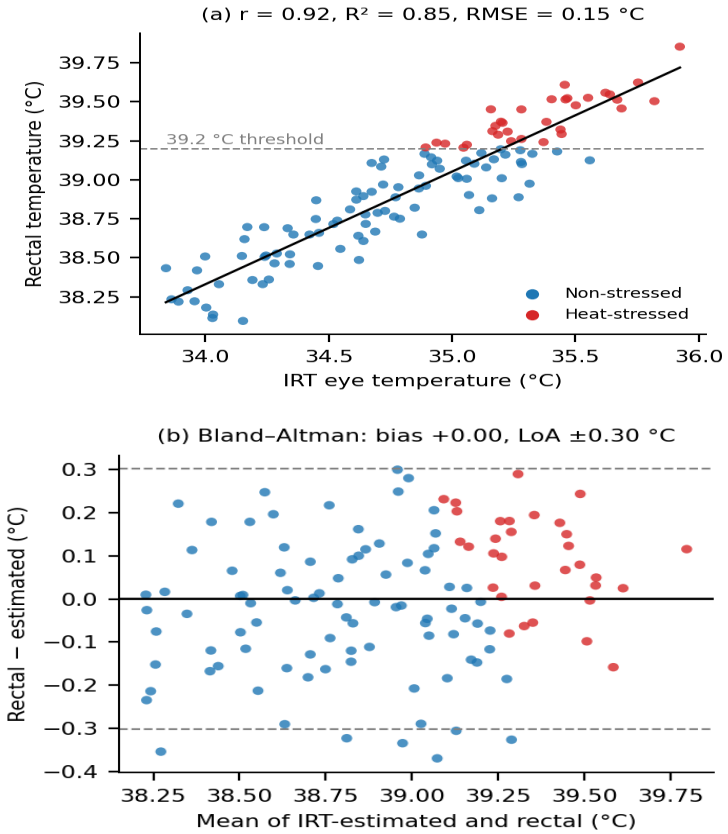


Fig 4. Agreement Between IRT Eye Temperature and Rectal Temperature: (A) Cross-Validated Linear Relationship with the 39.2 °C Heat-Stress Threshold and (B) Bland–Altman Plot of The Estimation Error.

Diurnal Herd Response and Real-Time Monitoring

Continuous monitoring is where IRT provides most value for management. **Fig. 5** presents a 24-h profile in which fixed cameras at the parlour exit or feed alley provide frames that are processed on an edge device and aggregated every 15 min. THI exceeded the alert level of 72 for 15.0 h of the day and peaked at 87.4 at 15:30. Herd-mean eye temperature rose from a night-time baseline of 34.6 °C to 35.7 °C at 19:45, and the share of animals flagged by the classifier peaked at 77 %. The cross-correlation between THI and herd eye temperature was highest (r = 0.98) at a lag of 2.25 h, and the thermal peak trailed the THI peak by about four hours, reflecting heat accumulation in body tissues. Eye temperature also fell back to baseline only after midnight, indicating incomplete overnight recovery. Two management consequences follow: the lag provides a window of roughly two hours between an environmental alert and a measurable body response in which cooling can be started pre-emptively, and cooling should be continued into the evening because animals remain heat-loaded after THI has fallen.

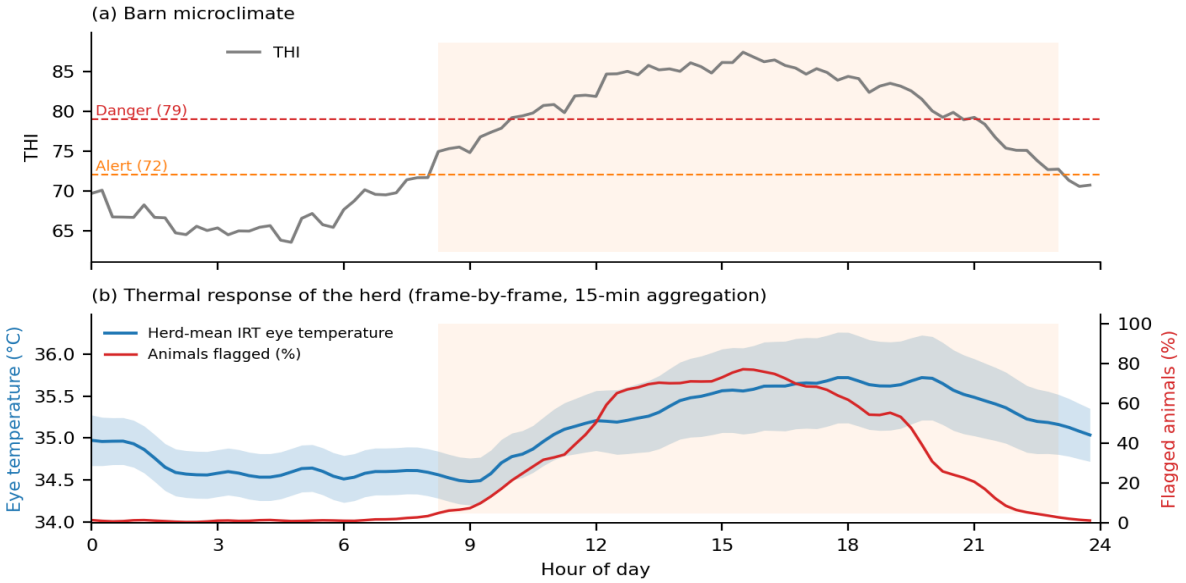


Fig 5. Simulated 24-H Monitoring: (A) Barn THI with Alert (72) and Danger (79) Levels and (B) Herd-Mean IRT Eye Temperature (±1 SD) With the Percentage of Animals Flagged as Heat-Stressed. The Shaded Band Marks THI ≥ 72.

Classification of Heat-Stressed Animals

Table 3 and **Fig. 6** compare three logistic models under five-fold cross-validation. THI alone separated stressed from non-stressed animals poorly (AUC = 0.75; recall = 0.19), confirming that environmental indices cannot resolve individual differences within a herd. Eye temperature alone raised the AUC to 0.92. The combined model (Eq. 8) gave the best overall performance, with accuracy 0.84, precision 0.74, recall 0.63, F1 = 0.68 and AUC = 0.92. The confusion matrix shows 81 true negatives, 7 false positives, 12 false negatives and 20 true positives, i.e. a specificity of 0.92 and a sensitivity of 0.63. The moderate sensitivity at the default 0.5 probability cut-off is a decision-threshold issue rather than a limit of the data: since a missed case costs more than a false alarm on a farm, the ROC curve indicates that sensitivity can be raised by lowering the cut-off at the price of more false positives.

Table 3. Five-Fold Cross-Validated Performance of the Heat-Stress Classifiers

Sample	Predictors	Accuracy	Precision	Recall	F1-score	AUC
1	IRT eye + THI	0.84	0.74	0.63	0.68	0.92
2	IRT eye + THI	0.85	0.76	0.65	0.70	0.93
3	IRT eye + THI	0.83	0.73	0.62	0.67	0.91
4	IRT eye + THI	0.86	0.77	0.67	0.72	0.94
5	IRT eye only	0.82	0.70	0.59	0.64	0.92
6	IRT eye only	0.81	0.69	0.58	0.63	0.91
7	IRT eye only	0.83	0.72	0.61	0.66	0.92
8	IRT eye only	0.80	0.68	0.57	0.62	0.90
9	THI only	0.72	0.46	0.19	0.27	0.75
10	THI only	0.73	0.48	0.21	0.29	0.76
11	THI only	0.71	0.45	0.18	0.26	0.74
12	THI only	0.74	0.49	0.22	0.30	0.77

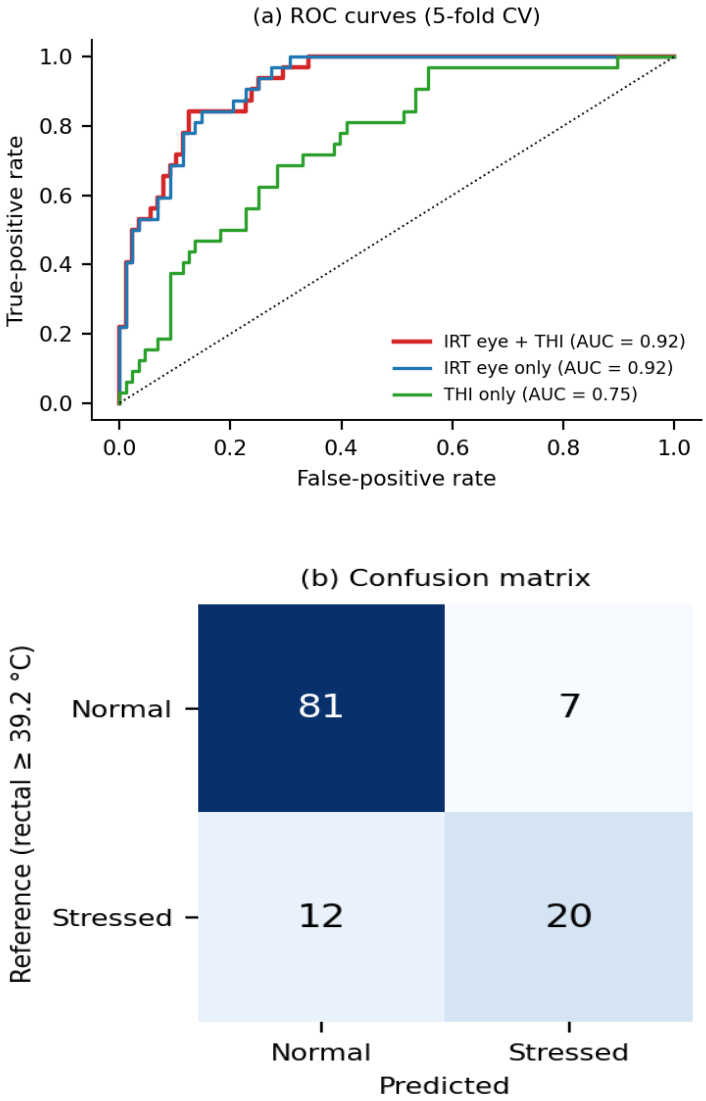


Fig 6. Classifier Performance: (A) ROC Curves for IRT Eye Temperature, THI and Their Combination and (B) Confusion Matrix of the Combined Model.

Implications for Climate-Resilient Farm Management

The results support a tiered decision protocol (**Table 4**) in which THI provides the early warning and IRT confirms which animals, and how much of the herd, are actually heat-loaded. This turns cooling from a calendar-based routine into a response-based one: sprinklers and fans are run when and where the animals need them, saving water and electricity during periods of scarcity, while flagged individuals are examined and treated early. Over a season, herd-level thermal records document how well shade, ventilation and cooling investments perform, identify animals that are consistently resilient for selection decisions, and quantify the exposure that future climate scenarios impose on a given shed design. Because productivity losses caused by heat stress and the emissions intensity of milk are linked [2], protecting animals from heat also contributes to efficient, lower-emission production.

Table 4. Proposed Tiered Alert Protocol Combining THI and IRT Outputs (Thresholds to Be Tuned Locally)

Tier	Trigger	Recommended action
1 Watch	THI ≥ 72 or herd-mean TSI > 1	Ensure shade and clean drinking water; switch on fans; avoid handling during midday
2 Alert	THI ≥ 79 or ≥ 25 % of animals flagged	Start sprinkler–fan cycles; shift feeding to cooler hours; postpone transport and vaccination
3 Emergency	≥ 50 % flagged or any animal with TSI > 3	Continuous cooling into the night; inspect flagged animals and call the veterinarian; reduce stocking density

Limitations

The numerical results presented here are simulated and should be substantiated by measured results in a number of breeds, coat colours, lactation stages and seasons. The accuracy of the camera (±2 °C) exceeds the changes of interest, and hence, relative changes (as in Eq. (6)) are more likely to be accurate than absolute changes. Standardisation of procedures and shaded imaging stations are needed for control of solar loading, wet or dirty coats, imaging angle and distance, and wind effects, which are potential sources of bias in skin temperature measurements. Finally, a fixed camera deployment needs to know which animal the camera is deployed on before per-animal alerts can be given (e.g. by using an RFID tag, or coat pattern recognition).

V. CONCLUSION

The proposed infrared thermography (IRT)-based pipeline incorporates the radiometric correction, automatic image segmentation, standardized thermal stress indices, and barn temperature-humidity index (THI) measurement to provide a non-invasive method for measuring heat stress in cattle at the herd scale. Eye temperature was shown to be consistent with rectal temperature with a root mean square error (RMSE) of 0.15 °C in the demonstration dataset and with a combination of eye temperature and THI the area under the receiver operating characteristic curve (AUC) for heat stress classification was 0.92, compared to 0.75 when using only THI. The results suggest some value in combining measures at the animal level with environmental measures to better identify heat risks. In addition, the 2.25 h delay between changes in THI and herd thermal response, as well as incomplete night-time recovery suggests the need to account for both delayed physiological responses and cumulative heat exposure when deciding when to initiate and terminate a cool. Such a multi-stage approach to decision support, built on these outputs, could support farmers in prioritizing interventions for the betterment of animal welfare and the most efficient use of water and energy. The reported results, however, must be taken with the grain of salt of the demonstration data set and must be tested separately in the field. The framework will be tested with measured multi-breed datasets under a range of climatic and management conditions in the future; detection and classification models will be developed for use on computers with low-cost hardware; and correlations between thermal recordings, milk production and reproductive performance will be explored. This would facilitate sustainable and scalable data-based livestock management, which is climate-friendly.

CRediT Author Statement

The author reviewed the results and approved the final version of the manuscript.

Data Availability

No data was used to support this study.

Conflicts of Interests

The authors declare no conflict of interest.

Funding

No funding agency is associated with this research.

Competing Interests

There are no competing interests.

References

[1]. M. G. Ciliberti, M. Albenzio, and A. Sevi, “From Sensors to Sustainability: Integrating Welfare, Management, and Climate Resilience in Small Ruminant Farm Systems,” Animals, vol. 15, no. 22, p. 3240, Nov. 2025, doi: 10.3390/ani15223240.
[2]. A. P. Nugroho et al., “Development of a low-cost thermal imaging system for water stress monitoring in indoor farming,” Smart Agricultural Technology, vol. 11, p. 101048, Aug. 2025, doi: 10.1016/j.atech.2025.101048.
[3]. A. I. Hazmy et al., “Potential of Satellite-Airborne Sensing Technologies for Agriculture 4.0 and Climate-Resilient: A Review,” IEEE Sensors Journal, vol. 24, no. 4, pp. 4161–4180, Feb. 2024, doi: 10.1109/jsen.2023.3343428.
[4]. S. Kundu, D. K. Saini, R. K. Meena, R. N. Bahuguna, and S. V. K. Jagadish, “High-throughput phenotyping and AI technologies for deciphering crop resilience to heat stress,” Plant Physiology Reports, vol. 29, no. 4, pp. 699–715, Nov. 2024, doi: 10.1007/s40502-024-00821-4.
[5]. M. Awais et al., “UAV-based remote sensing in plant stress imagine using high-resolution thermal sensor for digital agriculture practices: a meta-review,” International Journal of Environmental Science and Technology, vol. 20, no. 1, pp. 1135–1152, Jan. 2022, doi: 10.1007/s13762-021-03801-5.
[6]. M. Smigaj et al., “Thermal Infrared Remote Sensing of Stress Responses in Forest Environments: a Review of Developments, Challenges, and Opportunities,” Current Forestry Reports, vol. 10, no. 1, pp. 56–76, Dec. 2023, doi: 10.1007/s40725-023-00207-z.
[7]. E. B. Rebez, V. Sejian, M. V. Silpa, and F. R. Dunshea, “Heat Stress and Histopathological Changes of Vital Organs: A Novel Approach to Assess Climate Resilience in Farm Animals,” Sustainability, vol. 15, no. 2, p. 1242, Jan. 2023, doi: 10.3390/su15021242.
[8]. A. Noman Mahin, N. Adnan, and R. Khondoker, “Precision Agriculture using Machine Learning and Deep Learning Algorithms: A Comprehensive Study,” Journal of Agriculture & Education Research, vol. 04, no. 01, pp. 01–29, Jan. 2026, doi: 10.64030/3065-8764.04.01.01.
[9]. E. Rebez et al., “Applications of Artificial Intelligence for Heat Stress Management in Ruminant Livestock,” Sensors, vol. 24, no. 18, p. 5890, Sep. 2024, doi: 10.3390/s24185890.

[10]. V. Sejian, C. G. Shashank, M. V. Silpa, A. P. Madhusoodan, C. Devaraj, and S. Koenig, "Non-Invasive Methods of Quantifying Heat Stress Response in Farm Animals with Special Reference to Dairy Cattle," Atmosphere, vol. 13, no. 10, p. 1642, Oct. 2022, doi: 10.3390/atmos13101642.
[11]. W. Ashfaq, G. Brodie, S. Fuentes, and D. Gupta, "Infrared Thermal Imaging and Morpho-Physiological Indices Used for Wheat Genotypes Screening under Drought and Heat Stress," Plants, vol. 11, no. 23, p. 3269, Nov. 2022, doi: 10.3390/plants11233269.
[12]. M. D. Ghezzi et al., "Utilization of Infrared Thermography in Assessing Thermal Responses of Farm Animals under Heat Stress," Animals, vol. 14, no. 4, p. 616, Feb. 2024, doi: 10.3390/ani14040616.
[13]. C. Kaya, "Metabolomics-guided engineering of drought-resilient crops: Integrating multi-omics and AI for climate-smart agriculture," Plant Science, vol. 365, p. 113025, Apr. 2026, doi: 10.1016/j.plantsci.2026.113025.
[14]. H. T. Nguyen et al., "Advancing Crop Resilience Through High-Throughput Phenotyping for Crop Improvement in the Face of Climate Change," Plants, vol. 14, no. 6, p. 907, Mar. 2025, doi: 10.3390/plants14060907.
[15]. A. Joy et al., "Non-invasive measure of heat stress in sheep using machine learning techniques and infrared thermography," Small Ruminant Research, vol. 207, p. 106592, Feb. 2022, doi: 10.1016/j.smallrumres.2021.106592.
[16]. Rehman, Z. Ahmad, M. Ramakrishnan, R. Kalendar, and Q. Zhuge, "Regulation of plant epigenetic memory in response to cold and heat stress: towards climate resilient agriculture," Functional & Integrative Genomics, vol. 23, no. 4, Sep. 2023, doi: 10.1007/s10142-023-01219-5.

Publisher's note: The publisher remains neutral with regard to jurisdictional claims in published maps and institutional affiliations. The content is solely the responsibility of the authors and does not necessarily reflect the views of the publisher.

ISSN: 3104-4654